Synchrotron-based FTIR spectra of stained single cells. Towards a clinical application in pathology

Jacek Pijanka[1], Ganesh D Sockalingum[2], Achim Kohler[3,4], Ying Yang[1], Florence Draux[2], Gary Parkes[5], Ka-Po Lam[6], Dave Collins[6], Paul Dumas[7], Christophe Sandt[7], Daniel G van Pittius[5], Gill Douce[5], Michel Manfait[2], Valérie Untereiner[2] and Josep Sulé-Suso[1,8]

Over the last few years, FTIR spectroscopy has become a potential analytical method in tissue and cell studies for cancer diagnosis. This has opened a way towards clinical applications such as a tool that would scan samples to assess the presence or absence of malignant cells in biopsies, or as an aid to help pathologists to better characterise those cells that are suspicious but not diagnostic for cancer. The latter application has the problem that in order to assess these cells pathologists would have already dealt with stained samples. Therefore, it is important to understand how staining would affect the spectra of cells. To this purpose, we have conducted this study in order to clarify, first, how haematoxylin and eosin (H&E) and Papanicolau (Pap) stainings affect the spectra of single cells and, second, whether FTIR spectroscopy could differentiate between stained lung cancer cells and their normal counterparts. Furthermore, different cell preparations (cytospin, and smear) used in cytological diagnosis were assessed. Experiments performed using a bright infrared (IR) source (synchrotron) showed that both H&E and Pap staining induced marked changes in the lipid and amide-II band regions. Despite this, FTIR spectroscopy of already stained cells is capable of differentiating between lung cancer cells and their normal counterparts. The clinical applications of this methodology are discussed.
Laboratory Investigation (2010) **90,** 797–807; doi:10.1038/labinvest.2010.8; published online 1 February 2010

It is widely accepted that FTIR spectroscopy has a high potential to become a tool for cancer diagnosis. It uses an infrared (IR) beam that, after interacting with the sample, gives highly informative molecular information. Also, spatially resolved biochemical information from cells and tissue samples can be obtained by mapping or imaging techniques. In IR spectroscopy, the frequency of light that is absorbed by a sample depends upon the nature of the bond between the atoms, the atoms involved in the bond, and the type of vibration. The amount of light absorbed by a vibrating bond is linearly related to concentration. Therefore, the IR spectrum of a sample is a direct indicator of its chemical composition. Several studies have shown that FTIR spectroscopy can detect differences between cancer cells and their normal counterparts.[1] The applications could be twofold, as a tech-

nique that could screen tissue or cytology samples for the presence or absence of cancer cells, or as a tool that pathologists could use to better characterise individual cells that are suggestive but not diagnostic for malignancy. However, it is important that these clinical applications are not only based on robust algorithms but also should be fast and easily amenable to a Pathology laboratory setup. Obviously, further work will be required to assess the feasibility and what could be the time limit to provide a diagnosis. Nevertheless, in order to take this technique into its clinical application, the spectral biomarkers for cancer diagnosis need first to be characterised. Up to now, this work has entailed in most cases obtaining the spectra of unstained cells and/or tissue samples. Once the spectra are obtained, the same sample or a mirror sample as in the case of tissue, would be stained in order to

[1]Institute for Science and Technology in Medicine, Guy Hilton Research Centre, Keele University, Stoke on Trent, UK; [2]MéDIAN, Université de Reims Champagne-Ardenne, CNRS UMR6237-MEDyC, UFR de Pharmacie, IFR 53, Reims cedex, France; [3]Centre for Biospectroscopy and Data Modeling, Matforsk Nofima Food, Osloveien, Norway; [4]CIGENE, Center for Integrative Genetics, IMT, University of Life Sciences, Norway; [5]Department of Histopathology, Central Pathology Laboratory, University Hospital of North Staffordshire, Stoke on Trent, UK; [6]School of Computing and Mathematics, Keele University, Staffordshire, UK; [7]SOLEIL Synchrotron, BP48, L'Orme des Merisiers, Gif sur Yvette cedex, France and [8]Cancer Centre, University Hospital of North Staffordshire, Stoke on Trent, UK
Correspondence: Dr J Sulé-Suso, MD, PhD, Institute for Science and Technology in Medicine, Keele University, Guy Hilton Research Centre, Thornburrow Drive, Stoke on Trent, Staffordshire ST4 7QB, UK.
E-mail: jsule@dial.pipex.com

correlate the spectra with histopathological diagnosis.[2,3] However, this presents the problem that, a priori, it is not always possible to assess the presence of malignant cells through cytology or in a tissue sample before staining. Therefore, a large number of samples need to be studied with FTIR spectroscopy in order to build a database of spectral biomarkers for tissue/cell diagnosis. On the other hand, it is not unusual to have biopsy samples with small number of cells deemed suspicious but not diagnostic for cancer. In these cases, patients have to undergo further biopsies with all the risks, side effects, and costs that this entails. Therefore, a technique that could further characterise these already stained 'abnormal' cells would be of great interest. To our knowledge, the only study of FTIR spectra obtained from stained samples was conducted by Dukor[4] using breast tissue sections mounted on a glass slide and studied with FTIR-attenuated total reflectance (ATR) microspectroscopy. However, when bringing the sample close to an ATR crystal, care had to be taken to prevent glass interfering with the sample's FTIR spectra.[4] Furthermore, it is more difficult to obtain FTIR spectra of a single, chosen cell using ATR microspectroscopy when compared with FTIR microspectroscopy using transmission or reflection modalities.

One of the possible ways to improve this is to study both cytology and tissue samples already stained with haematoxylin and eosin (H&E), or Papanicolau (Pap), using FTIR spectroscopy in reflection and/or transmission modes. This would allow researchers to obtain FTIR spectra directly from those cells considered suspicious but not diagnostic for cancer. However, the problem lies in any spectral changes caused by the stains themselves and/or the procedure to stain these samples. To this purpose, we have conducted the present study in order to assess whether it was feasible to obtain good-quality FTIR spectra from already stained single cells. We studied both H&E- and Pap-stained cells as these two staining techniques are widely used in pathology departments. On the other hand, we chose to use Synchrotron-based FTIR (S-FTIR) microspectroscopy in view of its intrinsic high brightness, which allows to record high-quality spectra at diffraction-limited spot sizes. Synchrotrons are accelerator facilities that provide extremely high-flux and high-brightness electromagnetic radiation, at energies ranging from the IR through the ultraviolet to the X-ray regions. The use of synchrotron in IR microspectroscopy has allowed the study of biological samples at both cellular and subcellular levels.[5,6] Furthermore, synchrotron IR radiation is not damaging for cells.[7–9] The results presented here will lead to the study of already stained cell as well as tissue samples using FTIR spectroscopy, paving the way to the clinical application of FTIR spectroscopy in the diagnosis of cancer.

MATERIALS AND METHODS
Cell Lines
The lung epithelial cell line NL20 and the epidermoid lung cancer cell line Calu-1, purchased from the American Type Culture Collection (ATCC, LGC Standards, Teddington, UK) and the European Collection of Cell Cultures (ECACC, Salisbury, UK), respectively, were used in this study. NL20 cells were kept in culture in Ham's F12 (Lonza, UK) supplemented with 4% foetal calf serum, insulin, epidermal growth factor, transferrin, and hydrocortisone, according to the manufacturer's instructions. The Calu-1 cell line was kept in culture in DMEM with 10% foetal calf serum. Cells were incubated at 37°C in 5% CO_2 in tissue culture flasks (Sarstedt, Leicester, UK).

Cell Growth on MirrIR Low-e Microscope Slides
Cell growth on MirrIR low-e microscope slides (Kevley Technologies, Chesterland, OH, USA) has been described previously.[6] Briefly, cells growing in tissue culture flasks were detached before reaching confluence with trypsin/EDTA (Sigma, UK) and collected by centrifugation at 1200 r.p.m. for 7 min. The supernatant was removed and the cell pellet was resuspended in 5 ml of culture media. Cell viability was assessed using the trypan blue exclusion method. Cells were then seeded at a density of 5×10^4 cells in 200 μl of complete media on MirrIR low-e microscope slides and incubated for 24 h at 37°C and 5% CO_2. Cytospins were prepared by seeding 10^5 cells/ml on a cytospin funnel and spun at 1500 r.p.m. for 1 min onto a MirrIR low-e microscope slide, fixed, and allowed to dry. Smears were prepared by seeding 10^5 cells on MirrIR low-e microscope slides and spreading them out using a glass slide. They were then fixed and allowed to dry.

In order to confirm that exactly the same cells were studied with S-FTIR spectroscopy pre- and post-staining, a grid was drawn on MirrIR low-e microscope slides using a diamond pen (Figure 1). This method allowed the identification and localisation of each individual cell based on row and column numbers.
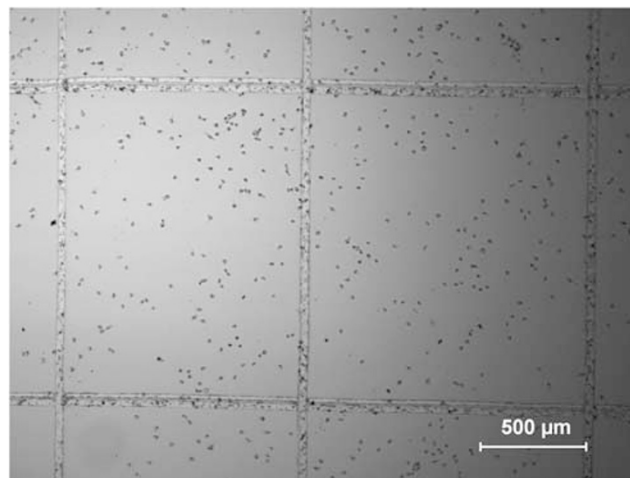

Figure 1 Image of an MirrIR low-e microscope slide with a grid drawn on it containing NL20 cells ($\times$ 4 magnification).

Cell Staining

Both normal and lung cancer cells were seeded on MirrIR low-e microscope slides as described above. After 24 h of incubation, the cells were washed and fixed as previously described.[6] Samples were then stained with either H&E or Pap using the same standard staining protocols at the Pathology Departments at the University Hospital of North Staffordshire (UHNS) and at the Reims University Hospital. The H&E staining process includes a first step of staining with haematoxylin and then eosin, while Pap staining includes staining with haematoxylin, Orange G, and EA50 in this order. More importantly, H&E staining includes one wash with ethanol after eosin staining but not after haematoxylin staining. However, Pap staining includes ethanol washes after haematoxylin, Orange G, and EA50 stains are added to the sample. This has important implications to understand some of the data presented here (*vide infra*).

S-FTIR Microspectroscopy

The S-FTIR spectra of Calu-1 and NL20 cells were recorded at the SMIS beamline at the SOLEIL Synchrotron facilities (Saint-Aubin, France). A Nicolet Nexus FTIR spectrometer coupled to a Nicolet Continuum XL IR microscope fitted with a × 32 infinity-corrected Schwarzschild objective and equipped with a liquid nitrogen-cooled MCT/A detector was used. The spectra were collected at 4-cm^{-1} resolution using a double-path single masking aperture size of $15 \times 15 \, \mu m^2$. The spectra were processed and corrected for Mie scatter using Extended Multiplicative Signal Correction.[10] Principal component analysis (PCA) of the whole spectral region was performed using The Unscrambler v9.8 (CAMO software AS, Oslo, Norway).

Statistical Analysis

The statistical properties of the data samples sets collected were examined using Student's *t*-test. To facilitate our analysis, characteristics of the sample spectra must somehow be described in the form of univariate distributions. Here, individual spectra representing independent measurements of a sample are investigated by means of the spectral similarity measure of SAM (Spectral Angle Mapper), which is widely used for material identification and image classification in the remote-sensing community.[11] Using SAM, our tests were constructed based on a mathematically vigorous framework
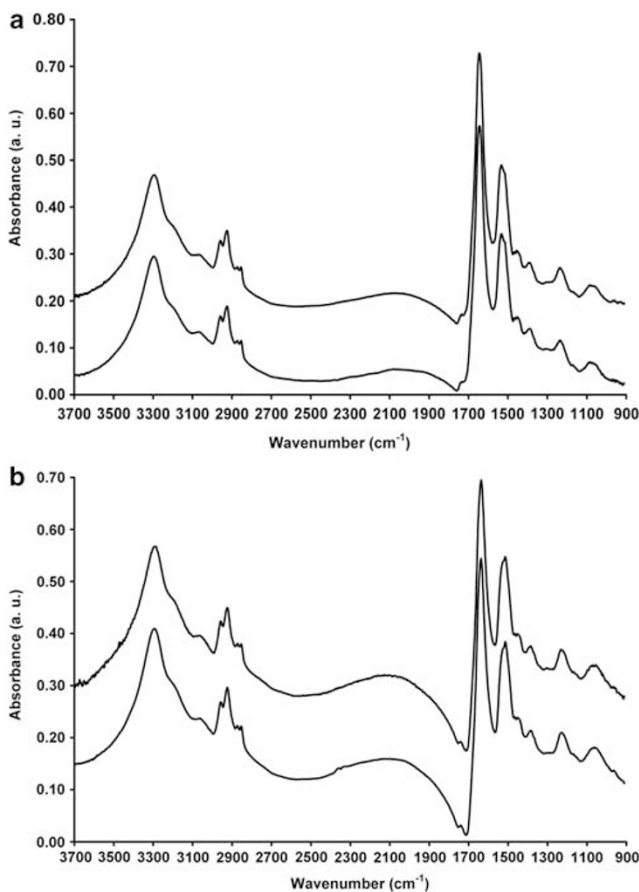

Figure 2 Mean S-FTIR spectrum of the same 50 individual control Calu-1 cells (**a**) and 50 NL20 cells (**b**) on day 1 (bottom spectrum) and on day 3 (top spectrum). The spectra are offset for clarity.
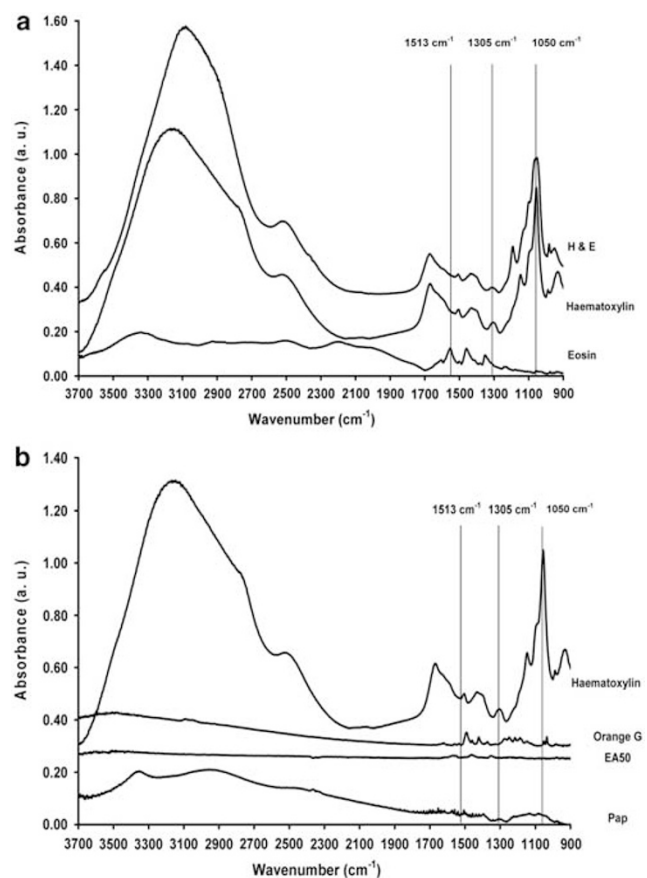

Figure 3 Mean of 10 S-FTIR spectra of H&E staining (**a**) and its individual components, and Pap staining (**b**) and its individual components. The spectra are offset for clarity.

of multi-spectral signatures, which determined the similarity of sample spectra by attributing a unique fingerprint, or reference signature, to the spectral responses or measurements of the individual sample set.[12] The advantages are four-fold: (1) SAM is insensitive to illumination measured at the individual spectral bands (or wavenumbers), particularly in cases of high data dimensionality ($\sim$1600 in our case), since the algorithm uses only the multidimensional vector direction and not its length. (2) While pattern classification and hypothesis testing address problems that are somewhat different, they are closely related under the formalism of SAM. (3) Broadly speaking, SAM shares the same data reduction principle of projection pursuit of which the widely used PCA method is a special case, while other, more sophisticated, component analytic procedures yield curved surfaces embedded in the full multidimensional space on to which arbitrary (spectral) patterns can be projected.[13,14] (4) The theoretical framework of SAM can readily be extended to incorporate advanced data analytics, including Spectral Information Divergence that has been shown to be more robust when the sample sizes are limited.[12]

Furthermore, the angular distances as measured by SAM between individual spectra (or measurements) of a sample

and its corresponding reference signature, followed a log-normal distribution (data not shown). Consequently, the logarithm function must first be applied to the random variable of the *t*-test procedure.

RESULTS

The aim of this study was to assess the effects of staining on the FTIR spectra of the same single lung cells pre- and post-staining and, thus conducted at different time points. Therefore, it was important for us to confirm spectra acquired from the same cells scanned at different days did not vary. To this purpose, we used control cells. First, we obtained the spectra of both NL20 and Calu-1 control cells on day 1, that is, the same day we collected the S-FTIR spectra of pre-stained cells. The control cells were then taken together with the other samples to be stained with either H&E or Pap at the Pathology Department at the Reims University Hospital. Unstained control cells were then taken back to the SOLEIL synchrotron and the S-FTIR spectra of exactly the same individual control cells were acquired again and in parallel to obtaining the spectra of stained cells. Figures 2a and b show, respectively, the mean S-FTIR spectra of control Calu-1 and NL20 cells obtained at different time points. PCA analysis
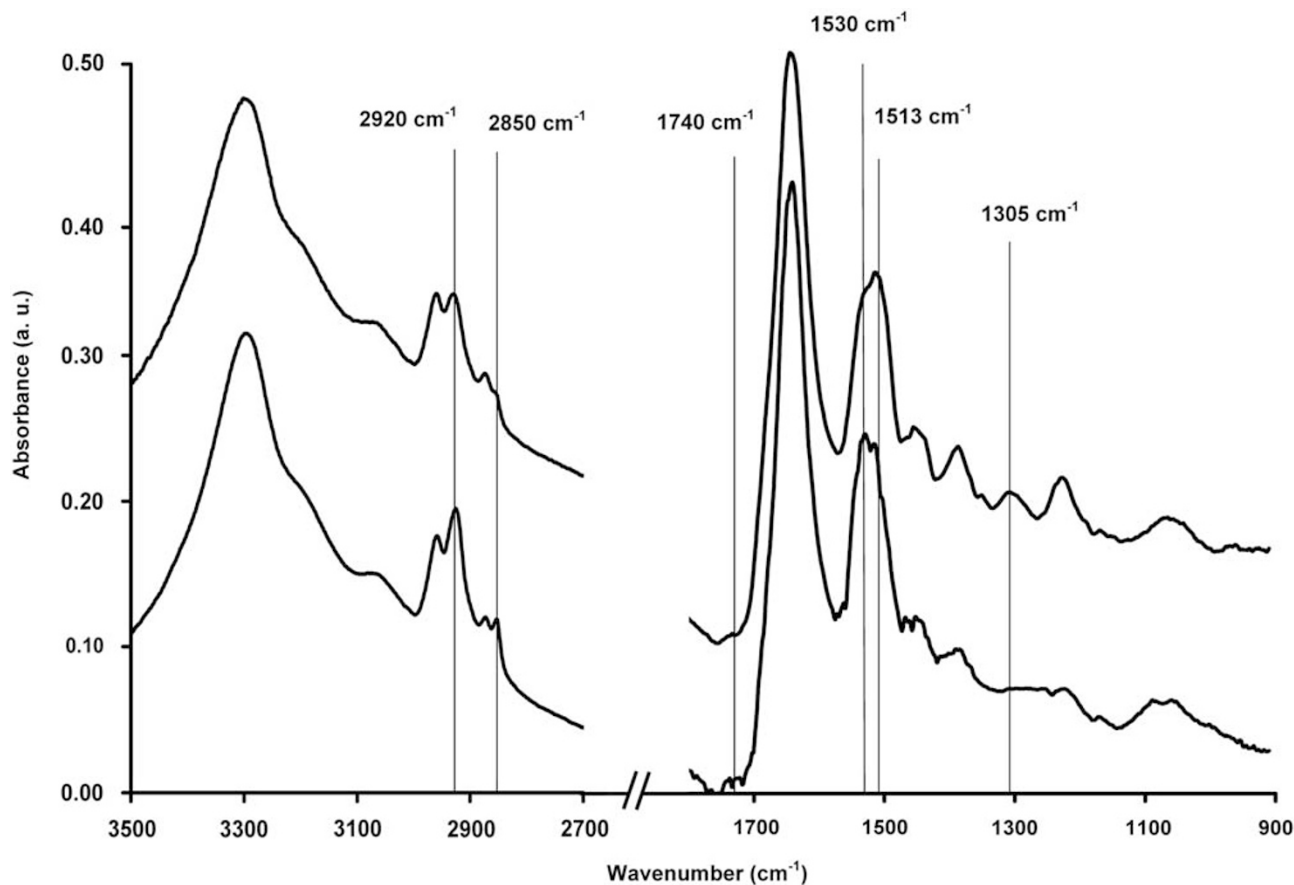

Figure 4 Mean S-FTIR spectrum of the same 50 individual Calu-1 cells pre-H&E staining (bottom spectrum) and post-H&E staining (top spectrum). The spectra are offset for clarity.
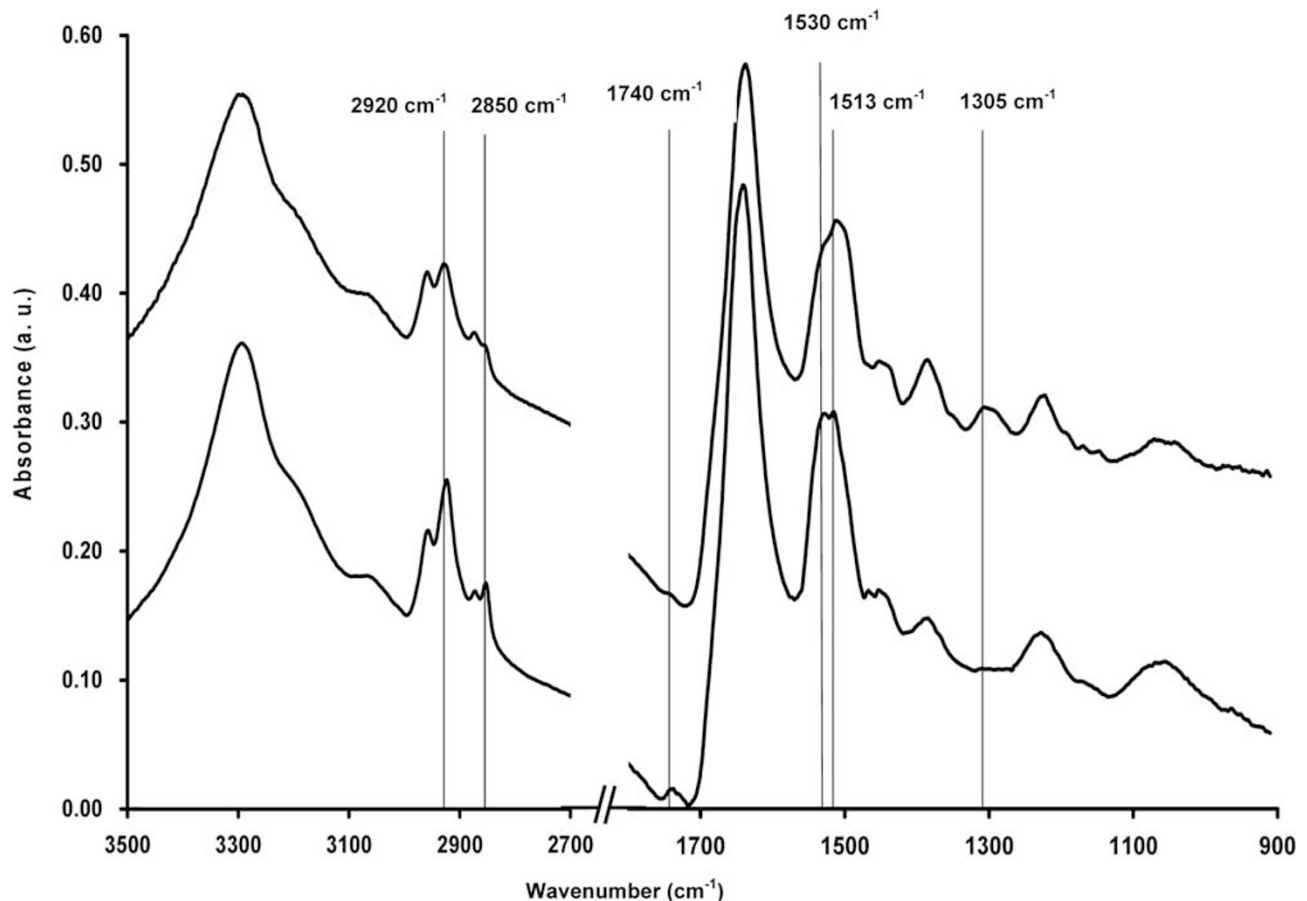
Figure 5 Mean S-FTIR spectrum of the same 50 individual NL20 cells pre-H&E staining (bottom spectrum) and post-H&E staining (top spectrum). The spectra are offset for clarity.

confirmed that there was no major difference between the spectra of Calu-1 cells obtained at different time points. Similarly, the same applied for NL20 cells. Also, no statistically significant differences were observed between the spectra of control Calu-1 and NL20 cells obtained at different time points ($P = 0.119$ for Calu-1 and $P = 0.892$ for NL20). On the other hand, we recorded reference spectra of both H&E and Pap stains (Figures 3a and b). The chemical compound responsible for the stronger peaks was haematoxylin in both H&E and Pap staining, with the strongest peak at $1050\,cm^{-1}$.

Following this preliminary work, we studied whether and how H&E and/or Pap staining could affect the spectra of both lung cancer and epithelial cells. H&E and Pap staining caused changes in the lipids and in the fingerprint area in the spectra of both cell lines (Figures 4–7). Regarding lipids, both staining procedures caused a decrease of the peaks around 2920 and $2850\,cm^{-1}$ in both study cell lines. In the fingerprint area, there was a decrease in the intensity of the band around $1740\,cm^{-1}$ in both cell lines following staining with either H&E or Pap. Also, there was a shift of the amide-II

band from around $1530\,cm^{-1}$ to $1513\,cm^{-1}$ in both Calu-1 and NL20 cell lines after staining with either H&E or Pap. Furthermore, a stronger band appeared around $1305\,cm^{-1}$ in both cell lines following staining with H&E (Figures 4 and 5). However, this band was less visible when cells were stained with Pap (Figures 6 and 7).

One of the conditions for FTIR spectroscopy to become a standard tool in cancer diagnosis is the confirmation that different samples prepared at different centres give the same information using the same instrument. To this purpose, we also performed H&E and Pap staining on both Calu-1 and NL20 cell lines prepared at the Histopathology Department at the UHNS (Stoke on Trent, UK). The aim was to compare, using S-FTIR spectroscopy, data obtained from the same type of cells but prepared at two different centres (UHNS and Reims University Hospital). Neither PCAs nor statistical analysis showed any differences when comparing H&E ($P = 0.485$) or Pap ($P = 0.417$)-stained NL20 cells at either centre and Calu-1 cells stained with Pap at either centre ($P = 0.33$). However, this was not the case for the spectra of Calu-1 cells stained with H&E, where we saw a statistically
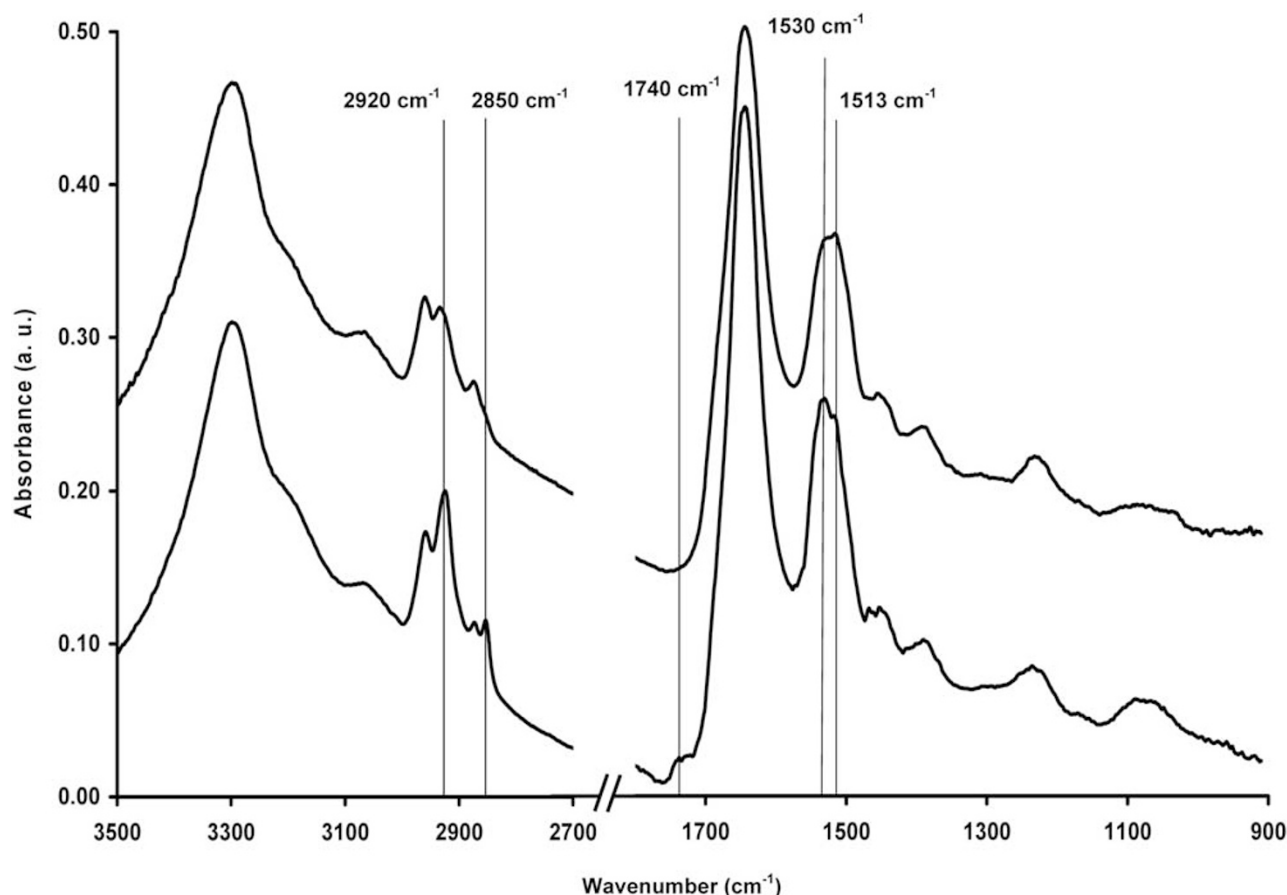
Figure 6 Mean S-FTIR spectrum of the same 50 individual Calu-1 cells pre-Pap staining (bottom spectrum) and post-Pap staining (top spectrum). The spectra are offset for clarity.

significant difference ($P = 0.031$) between samples prepared at UHNS and Reims University Hospital. This has important clinical implications as it emphasizes the importance of standardising the way samples are prepared.

Another important issue in pathology is the way samples are prepared for cytology, being in most cases cytospins or smears. While cytospins are more commonly used to study the presence of tumours in fluids (apart from urine), smears are used in fine-needle aspirations. Therefore, we studied whether S-FTIR spectroscopy could also be applied to cytology samples prepared in either cytospin or smear form that had already been stained with H&E or Pap. Figures 8 and 9 show the spectra of Calu-1 cells prepared either as a cytospin or smear, respectively. Interestingly, the peaks around 2850 and 2920 cm^{-1} decrease in intensity in either cytospin or smear samples that have been stained with Pap, but their intensity remains similar to that of control unstained samples when cytospins or smears are stained with H&E. Within the fingerprint area, the peak around 1740 cm^{-1} also disappeared when samples had been stained with Pap but not with H&E. Furthermore, while no major changes are seen in the amide-II peak when either cytospin or smear samples are stained

with H&E, staining with Pap caused a broadening of the amide-II peak.

The ultimate aim of such a study is to be able to differentiate between lung cancer cells and their normal counterparts following staining of each individual sample. To this purpose, we performed PCA analysis of the S-FTIR spectra of Calu-1 and NL20 cells following staining with either H&E or Pap. As can be seen in Figures 10a and b, PCA analysis showed different clustering for each cell line, which was clearer when cells were stained with Pap. Statistical analysis confirmed a difference between Calu-1 cells and NL20 cells stained with either H&E ($P = 0.012$) or Pap ($P = 0.00003$). Furthermore, PCA analysis also showed some clustering between unstained Calu-1 and NL20 cells (Figure 11), which was statistically significant ($P = 0.0012$).

DISCUSSION

One of the problems faced by pathologists when dealing with cancer diagnosis is assessment of the presence of cancer cells in those samples (cytology and/or tissue) that contain either a small number of cells, or abnormal cells considered suggestive but not diagnostic for cancer. It could be hypothesised
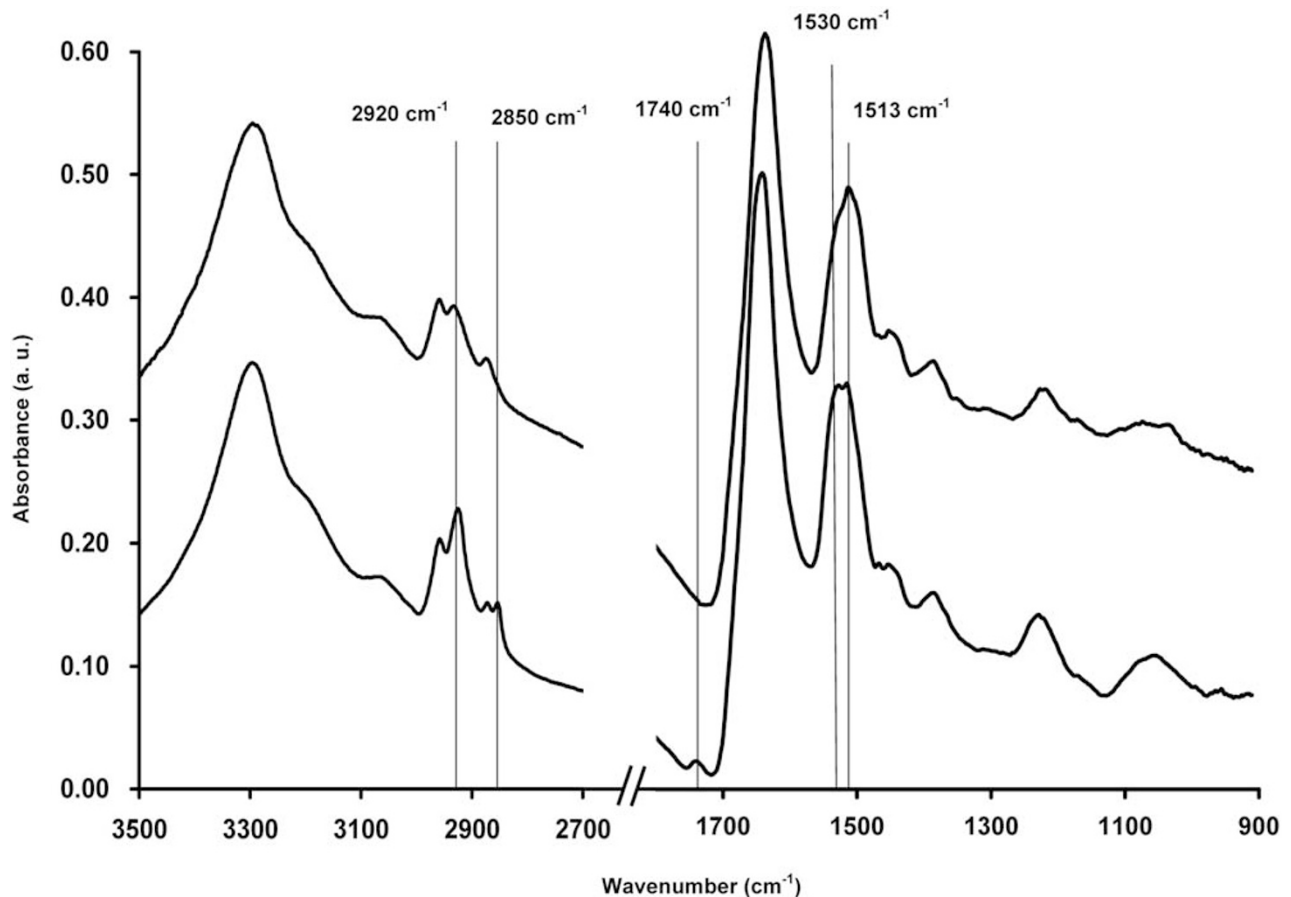
Figure 7 Mean S-FTIR spectrum of the same 50 individual NL20 cells pre-Pap staining (bottom spectrum) and post-Pap staining (top spectrum). The spectra are offset for clarity.

that spectral markers present in cancer cells might also be present, albeit in smaller intensity, in cells that could be suggestive but not diagnostic of cancer. Therefore, a tool that could study and further characterise single cells, helping pathologists to reach a diagnosis, would be highly welcomed. However, this needs to be achieved with already stained samples as it is not possible without staining to figure out which cytology and/or tissue samples could pose such a diagnostic problem.

So far, FTIR spectroscopy using synchrotron or bench-top spectrometers has concentrated on the study of dried or fixed cells,[15,16] and tissue either frozen,[17,18] in paraffin,[18,19] deparaffinised,[3,20] or prepared by touch-imprint cytology.[21] However, in all these cases, samples had been studied without prior staining. Therefore, from the pathologist point of view, it would be easier to have a tool that could characterise cells in already stained samples. One of the problems to achieve this is to know how stains could affect the FTIR spectra and whether such a methodology would be feasible. In order to answer this question, we recorded the S-FTIR spectra of single lung cancer cells and their normal counterparts, lung epithelial cells, prior to and following staining with either H&E or Pap.

To conduct this work, it was vital to obtain S-FTIR spectra from exactly the same individual cells pre- and post-staining. To do this, cells were cultured on MirrIR low-e slides onto which a grid had manually been drawn (Figure 1). Unstained cell samples were taken to the SOLEIL Synchrotron facilities and their S-FTIR spectra obtained. Following this, samples were stained at the Pathology Department at Reims University Hospital. However, this posed the problem to figure out whether any differences in the spectra of single cells pre- and post-staining were indeed due to staining or to the transportation of samples from SOLEIL synchrotron to Reims University Hospital and back to SOLEIL synchrotron. Furthermore, although the stability of the beam at the SOLEIL synchrotron is such that the same sample should have the same S-FTIR spectra obtained at different time points, we also wished to confirm that this was the case and that no differences were found in the spectra of these cells caused by the fact that the S-FTIR spectra were obtained at different time points. As can be seen in Figures 2a and b, there were no differences in the S-FTIR spectra of the same individual cells for both NL20 and Calu-1 cells when spectra were obtained at different days. This observation was supported by both PCA and statistical analysis showing no differences ($P = 0.119$ for
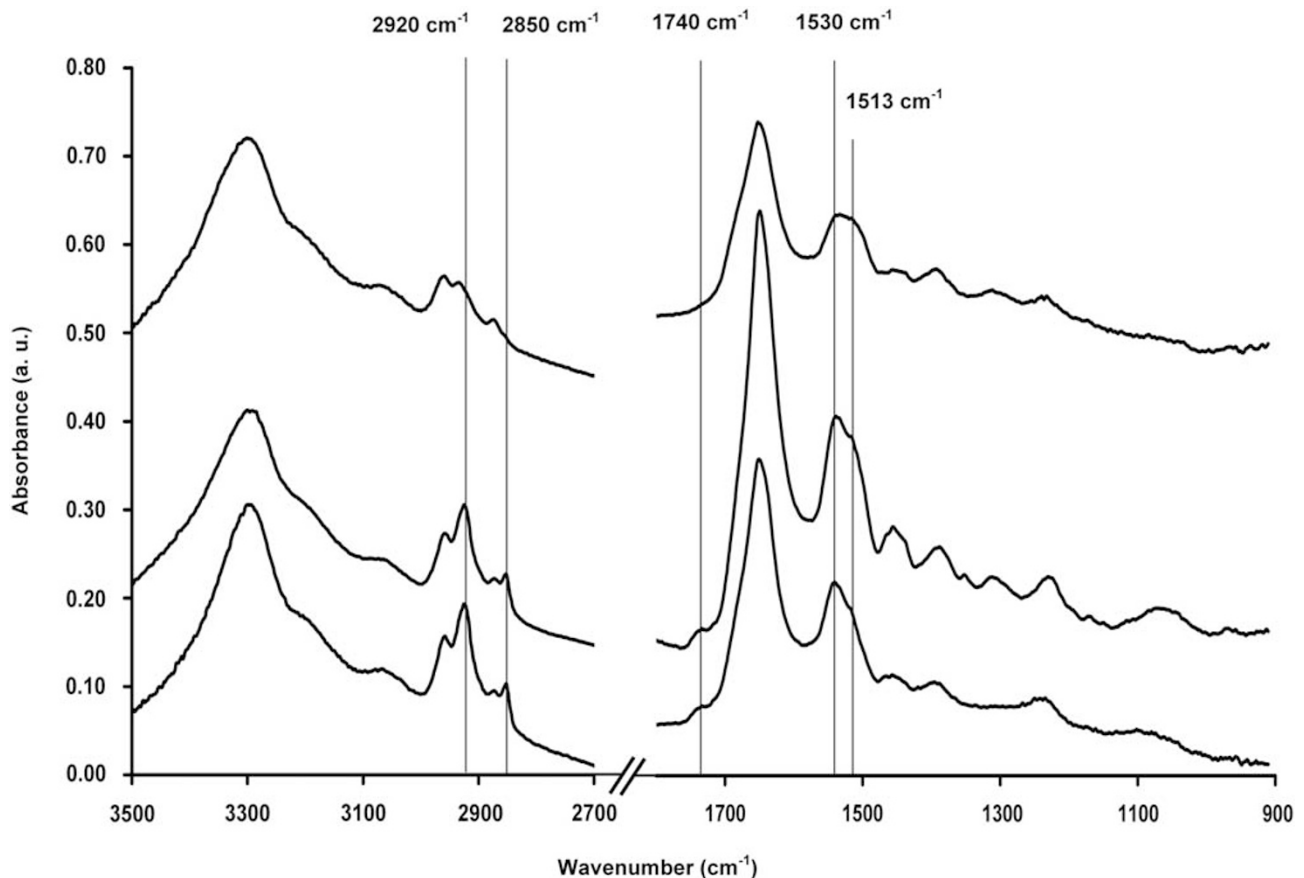
Figure 8 Mean S-FTIR spectrum of 50 individual Calu-1 cells as cytospin unstained (bottom spectrum), H&E-stained (middle spectrum), and Pap-stained (top spectrum). The spectra are offset for clarity.

Calu-1 and $P = 0.892$ for NL20). This preliminary work confirms that any possible differences between the spectra of both normal and lung cancer cells pre- and post-staining are not due to transportation or to changes in the synchrotron's beam stability.

The next step was to assess the effects of staining on the S-FTIR spectra of individual NL20 and Calu-1 cells. We used both H&E and Pap staining as these are widely used in histopathology, although Pap is more commonly used for cytology samples. Spectra of both stains (H&E and Pap) and of the different components of each stain showed that the strongest peaks were caused by haematoxylin, a component present in both staining techniques (Figures 3a and b). On this basis, we studied the changes in the spectra of both Calu-1 and NL20 cell lines following staining with H&E and Pap. As can be seen in Figures 4–7, the main changes in the lipid area correspond to disappearance of the peaks around 2850 and 2920 cm^{-1} in both cell lines and following staining with either H&E or Pap. The peaks at 2850 and 2920 cm^{-1} correspond mainly to the CH$_2$ stretching modes of the methylene chains in membrane lipids.[22–24] The use of ethanol in both H&E and Pap staining procedures would explain the decrease in the intensity of these two peaks.[15,16,25] This is further

confirmed by the fact that physical removal of membrane and cytoplasmic lipids caused a reduction in the intensity of these two peaks.[6] On the other hand, we did not see any differences in the bands around 2870 and 2960 cm^{-1}, which originate from the CH$_3$ groups not only of lipids and proteins, but also of nucleic acids.[23,26] In fact, physical removal of both membrane and cytoplasmic lipids does not cause changes in the intensity of those peaks.[6] Another change that can be associated with use of ethanol in both H&E and Pap staining procedures is the band at 1740 cm^{-1} (Figures 4–7). Absorptions in this spectral region arise from the carbonyl C=O stretching mode of phospholipids.[27,28] It has been described that upon washing with ethanol, phospholipids together with other membrane lipids are removed from the sample and thus their intensity decreases in the spectrum.[15] This corroborates the changes observed above for the CH$_2$ modes. Further changes were seen in the fingerprint region. As can be seen in Figures 4–7, the main changes were a shift of the amide-II band to lower wavenumbers, and the appearance of a stronger band at around 1305 cm^{-1} in cells stained with H&E. It has been described previously that ethanol can cause changes in both amide bands and shifts to lower wavenumbers.[29] The fact that this shift occurred in the two cell
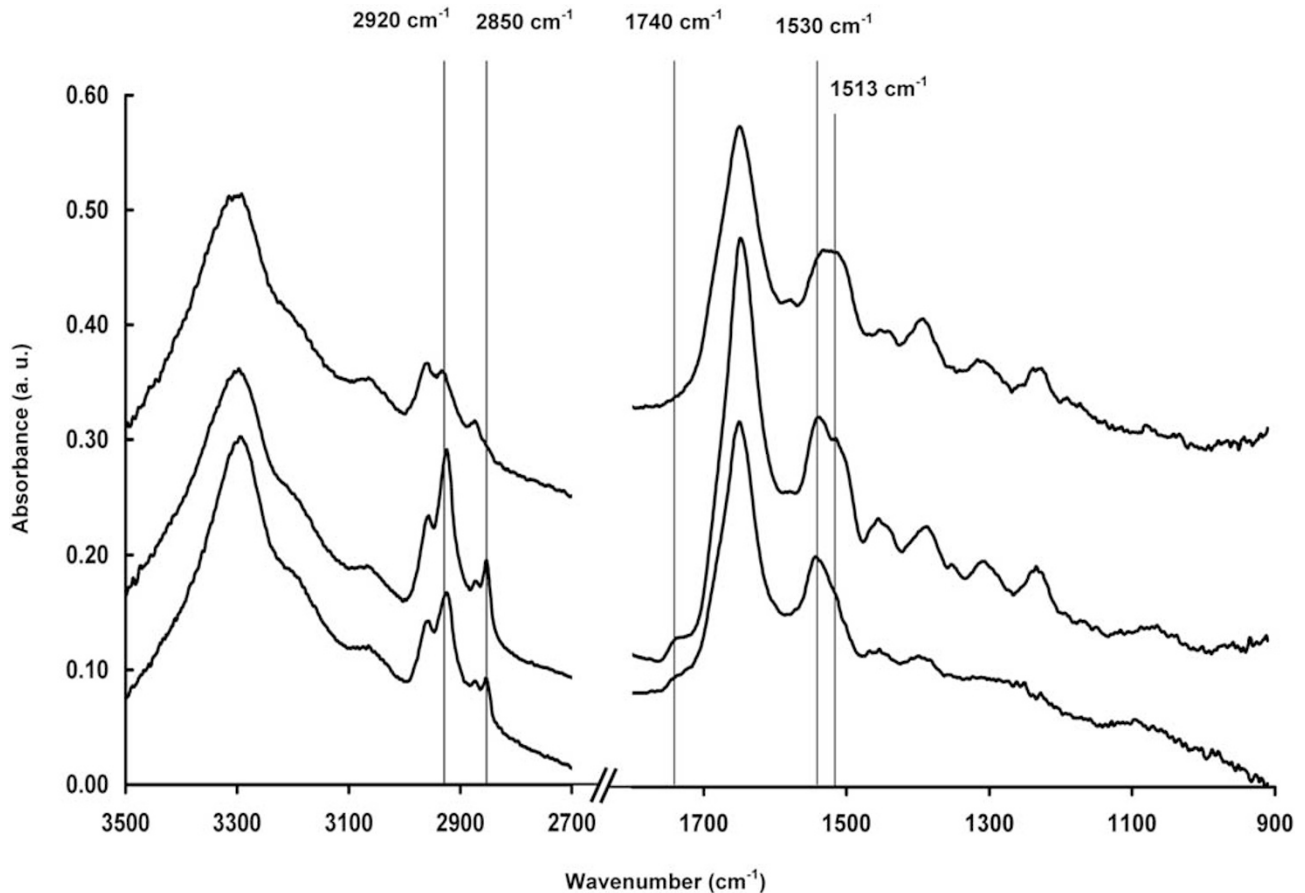
Figure 9 Mean S-FTIR spectrum of 50 individual Calu-1 cells as smear unstained (bottom spectrum), H&E-stained (middle spectrum), and Pap-stained (top spectrum). The spectra are offset for clarity.

lines and in both H&E- and Pap-stained samples would indicate that the shift is caused by the staining procedure rather than the stains themselves. This can be confirmed as haematoxylin, which causes the strongest peaks in both H&E and Pap, does not have a strong band at $1513\,cm^{-1}$ (Figures 3a and b). On the other hand, the region around $1305\,cm^{-1}$ is associated to the amide-III band.[30] However, the spectra of haematoxylin have a distinctive peak at $1305\,cm^{-1}$ (Figures 3a and b). While this peak is less intense when compared with other peaks such as $1050\,cm^{-1}$, we could assume that haematoxylin itself can contribute to the stronger intensity of the 1305-cm^{-1} peak. Furthermore, we do not see such a strong 1305-cm^{-1} peak in the spectra of cells stained with Pap. This may be explained by the fact that in this case, cells undergo three washings with ethanol, which could remove more haematoxylin from the final stain.

Another important issue in the development of FTIR spectroscopy as a tool to be used in the diagnosis of cancer is to confirm that samples stained at different pathology departments give similar spectra without any statistically significant differences. PCA and statistical analysis showed no differences in the spectra of Calu-1 and NL20 cells stained

with H&E or Pap at either the UHNS or the Reims University Hospital, apart from the case of Calu-1 cells stained with H&E where we saw a statistically significant difference ($P=0.031$). This shows that S-FTIR spectroscopy could detect differences in sample preparation not seen with a microscope. More important, it highlights that before such a technique could become standard in pathology, the way samples are prepared has to be highly standardised.

A further issue that may affect the spectral signatures of cells are the different ways cytology samples are prepared at the pathology departments. The most common methods are cytospin and smear. Therefore, it was important in this study to confirm that good FTIR spectra could be obtained from stained cytospin and smear samples. Figures 8 and 9 confirmed this observation. However, in the case of the lipid absorption area, while the 2850 and 2920-cm^{-1} bands decreased in intensity following staining with Pap, this was not the case following H&E staining. We have previously mentioned that disappearance of these two bands is due to the effect of ethanol on cells during the staining procedure. It is important to remember that H&E staining includes fewer steps involving ethanol washings than Pap staining.
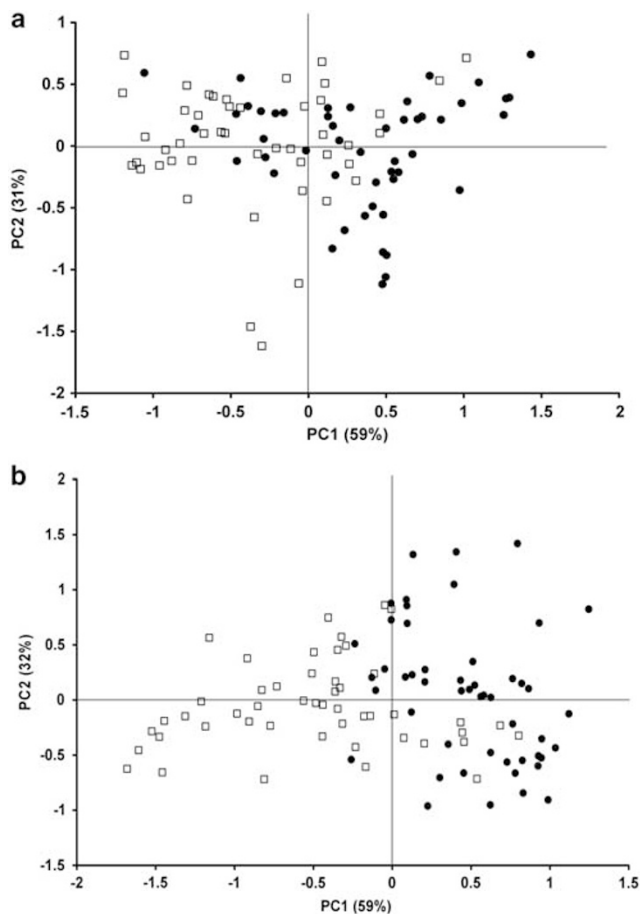
Figure 10 PCA analysis of the Calu-1 cell line (circles) and NL20 cell line (open squares) stained with H&E (**a**) or Pap (**b**).
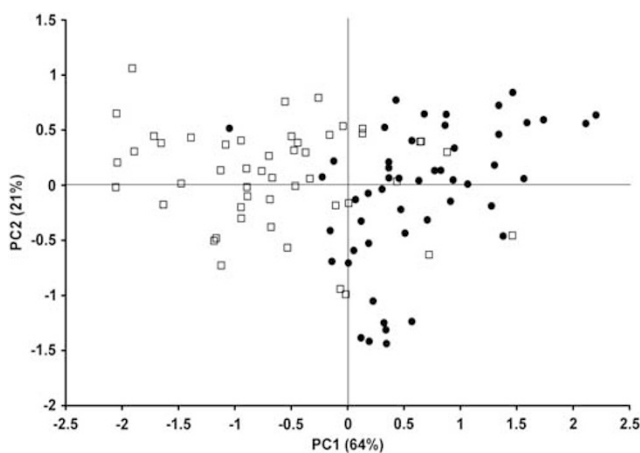

Figure 11 PCA analysis of the Calu-1 cell line (circles) and NL20 cell line (open squares) prior to staining.

Therefore, we can assume that the additional steps in the latter caused the decrease in the intensity of these bands. More importantly, this occurs for both cytospin and smear

samples, confirming that these changes are not due to sample preparation (cytospin *versus* smear) but rather the staining procedure itself. Similarly, the band around $1740\,cm^{-1}$ also decreases in intensity in cytospin and smear samples that have been stained with Pap, while no major changes were seen following H&E staining. The same reason for the changes in the lipid CH_2 absorption range can be applied to explain the changes in the $1740\text{-}cm^{-1}$ band. It has been described previously that ethanol may remove lipids that have not been appropriately fixed by formalin.[16] While the fixation protocol of cells growing on MirrIR low-e microscope slides was the same as the fixation protocol for cytospins and smears, it could be argued that fixation of lung cancer cells might have been more successful in the case of cytospin and smear rather than in the case of cancer cells growing on MirrIR low-e microscope slides.

Finally, if this technique is to make it to clinical practice as a diagnostic tool in pathology, it has to be able to differentiate between cancer cells and their normal counterparts. The data presented here show this is the case even for stained samples. This was confirmed not only with PCAs (Figures 10 and 11) but also with *t*-test, which showed a statistically significant difference between lung cancer cells and lung epithelial cells stained with H&E ($P = 0.012$), or Pap ($P = 0.00003$), and unstained ($P = 0.0012$) cells. The data presented here confirm the potential of this technique in cancer diagnosis. Further work is now being conducted to assess whether similar spectra can be obtained from the same stained samples using bench-top spectrometers. The latter will be a logical step to bring this technique to pathology departments to be used in the diagnosis of cancer.

DISCLOSURE/CONFLICT OF INTEREST
The authors declare no conflict of interest.

1. Andrus PG. Cancer monitoring by FTIR spectroscopy. Technol Can Res Treat 2006;5:157–167.
2. Lasch P, Haensch W, Naumann D, et al. Imaging of colorectal adenocarcinoma using FTIR microspectroscopy and cluster analysis. Biochim Biophys Acta 2004;1688:176–186.
3. Gazi E, Baker M, Dwyer J, et al. A correlation of FTIR spectra derived from prostate cancer biopsies with Gleason grade and tumour stage. Eur Urol 2006;50:750–761.
4. Dukor RK, Liebman MN, Johnson BL. A new, non-destructive method for analysis of clinical samples with DT-IR microspectroscopy. Breast cancer tissue as an example. Cell Mol Biol 1998;44:211–217.
5. Dumas P, Sockalingum GD, Sulé-Suso J. Adding synchrotron radiation to infrared microspectroscopy: what's new in biomedical applications? Trends Biotechnol 2007;25:40–44.

6. Pijanka J, Kohler A, Yang Y, *et al*. FTIR microscopy. Spectroscopic signatures of single, isolated cancer cell nuclei using synchrotron infrared microscopy. Analyst 2009;134:1176–1181.

7. Dumas P, Jamin N, Teillaud JL, *et al*. Imaging capabilities of synchrotron infrared microspectroscopy. Faraday Discuss 2004;126:289–302.

8. Holman H-YN, Bjornstad KA, McNamara MP, *et al*. Synchrotron infrared spectromicroscopy as a novel bioanalyticial microprobe for individual living cells: cytotoxicity considerations. J Biomed Opt 2002;7:417–424.

9. Martin MC, Tsvetkova NM, Crowe JH, *et al*. Negligible sample heating from synchrotron infrared beam. Appl Spectrosc 2001;55:111–113.

10. Kohler A, Sulé-Suso J, Sockalingum GD, *et al*. Estimating and correcting Mie scattering in synchrotron-based microscopic FTIR spectra by extended multiplicative signal correction (EMSC). Appl Spectrosc 2008;62:259–266.

11. Chang CI. Hyperspectral Imaging: Techniques for Spectral Detection and Classification. Kluwer Publishers: New York, NY, 2003.

12. Lam KP, Austin J, Day CR. A coarse-grained spectral signature generator. Proc SPIE 2007;6356:62560S1–62560S12.

13. Friedman JH, Tukey JW. A projection pursuit algorithm for exploratory data analysis. IEEE Trans Comp 1974;23:881–889.

14. Lam KP, Emery R. Image pixel guided tours – A software platform for non-destructive X-ray imaging. Proc SPIE/IS&T 2009;724:72450N1–72450N10.

15. Pacifico A, Chiriboga LA, Lasch P, *et al*. Infrared spectroscopy of cultured cells II. Spectra of exponentially growing, serum deprived and confluent cells. Vibr Spectrosc 2003;32:107–115.

16. Gazi E, Dwyer J, Lockyer NP, *et al*. Fixation protocols for subcellular imaging by synchrotron-based Fourier Transform Infrared Microspectroscopy. Biopolymers 2005;77:18–30.

17. Bird B, Miljkovic M, Romeo MJ, *et al*. Infrared micro-spectral imaging: distinction of tissue types in axillary lymph node histology. BMC Clin Pathol 2008;8:8.

18. Untereiner V, Piot O, Diebold M-D, *et al*. Optical diagnosis of peritoneal metastases by infrared microscopic imaging. Anal Bioanal Chem 2009;393:1619–1627.

19. Tfayli A, Piot O, Durlach A, *et al*. Discriminating nevus and melanoma on paraffin-embedded skin biopsies using FTIR microspectroccopy. Biochim Biophys Acta 2005;1724:262–269.

20. Bird B, Bedrossian K, Laver N, *et al*. Detection of breast micro-metastases in axillary lymph nodes by infrared micro-spectral imaging. Analyst 2009;134:1067–1076.

21. Das K, Kendall C, Isabelle M, *et al*. FTIR of touch imprint cytology: a novel tissue diagnostic technique. J Photochem Photobiol 2008;18:160–164.

22. Lasch P, Boese M, Pacifico A, *et al*. FT-IR spectroscopy investigations of single cells on the subcellular level. Vibr Spectrosc 2002;28:147–157.

23. Gao T, Feng J, Ci Y. Human breast carcinoma tissues display distinctive FTIR spectra: implications for the histological characterisation of carcinomas. Anal Cell Pathol 1999;18:87–93.

24. Zhou J, Wang Z, Sun S, *et al*. A rapid method for detecting conformational changes during differentiation and apoptosis of HL60 cell by Fourier Transform Infrared Spectroscopy. Biotechnol Appl Biochem 2001;33:127–132.

25. Beljebbar A, Amharref N, Lévèques A, *et al*. Modeling and quantifying biochemical changes in C6 tumor gliomas by Fourier Transform Infrared Imaging. Anal Chem 2008;80:8406–8415.

26. Neviliappan S, Fang Kan L, Tiang L, *et al*. Infrared spectral features of exfoliated cervical cells, cervical adenocarcinoma tissue and adenocarcinoma cell line (SiSo). Gynecol Oncol 2002;85:170–174.

27. Jamin N, Dumas P, Moncuit J, *et al*. Highly resolved chemical imaging of living cells by using synchrotron infrared microspectrometry. Proc Natl Acad Sci USA 1998;95:4837–4840.

28. Holman H-YN, Martin MC, Blakely EA, *et al*. IR spectroscopic characteristics of cell cycle and cell death probed by synchrotron radiation based Fourier transform IR spectromicroscopy. Biopolymers 2000;57:329–335.

29. Pleshko NL, Boskey AL, Mendelsohn R. An FTIR microscopic investigation of the effects of tissue preservation on bone. Calcif Tissue Int 1992;51:72–77.

30. Fujioka N, Morimoto Y, Takeuchi K, *et al*. Difference in infrared spectra from cultures cells dependent on cell-harvesting methods. Appl Spectrosc 2003;57:241–243.